Macromolecules
ARTICLE

Macromolecules **2010**, *43*, 765–771 **765**
DOI: 10.1021/ma902096p

Self-Organization and Excited-State Dynamics of a Fluorene−Bithiophene Copolymer (F8T2) in Solution

Rita França Rodrigues,[†] Ana Charas,[‡] Jorge Morgado,[‡] and António Maçanita*,[†]

[†]*Centro de Química Estrutural, Instituto Superior Técnico, Technical University of Lisbon, 1049-001 Lisboa, Portugal and* [‡]*Instituto de Telecomunicações, Instituto Superior Técnico, 1049-001 Lisboa, Portugal*

Received September 21, 2009; Revised Manuscript Received December 9, 2009

ABSTRACT: Poly(9,9-dioctylfluorene-*alt*-bithiophene) (F8T2) exhibits two distinct conformations in solution depending on the temperature and solvent. The transition from the high- to low-temperature conformation resembles the β-phase formation of poly(9,9-dioctylfluorene) (PFO), in the sense that there is an increase of the conjugation length, while involving less pronounced enthalpy and entropy changes ($\Delta H = -7.1$ kcal/mol and $\Delta S = -22.9$ cal/(mol K) vs $\Delta H = -18.0$ kcal/mol and $\Delta S = -68.4$ cal/(mol K) for PFO). The entropy loss indicates a substantial increase in the polymer order in the low-temperature conformation. Fluorescence decays of F8T2 in solvents with various viscosities, at different temperatures and collected at different emission wavelengths, are triple-exponential in character (e.g., 20, 440, and 650 ps in methylcyclohexane, at 20 °C). The two longer decay times are related to the lifetimes of the two conformations. The shorter decay time appears as either a decay or rise time, at the onset or the tail of the emission band, respectively, and is assigned to conformational relaxation on the basis of its dependence on solvent viscosity and temperature.

Introduction

Conjugated polymers represent a very promising alternative for flexible and large area electronics and optoelectronics applications.[1,2] Although fully operational prototypes exist already, there is still the need to further improve device performance and lifetime, increasing this technology competitiveness with respect to the traditional one, based on the inorganic semiconductors. In order to achieve this goal, a deeper understanding of the photophysics of conjugated polymers and the role of processing conditions and structural/molecular and supramolecular order are of key importance.

It is well established that the photophysical behavior of conjugated polymers depends on their intra- and/or interchain ordering. This ordering may be influenced by solvents, self-organization phenomena, and interactions arising in solid films. Polyfluorenes, one of the most studied conjugated luminescent polymer family, provide a good example for such variety of states. A particularly ordered state was first identified in poly(9,9-dioctylfluorene) (PFO, Chart 1), and designated by β-phase, where ordered chain segments/or domains coexist within the disordered bulk (α phase).[3−6] The observation of the β-phase in single PFO molecules[6] is quite remarkable. The β-phase has a clear spectroscopic signature: a narrow absorption peak at 438 nm and an unusually well-resolved fluorescence spectrum.[5] This process is translated by an equilibrium that involves intrachain ordering followed by aggregation and growth into the commonly named "hairy rod" blocks.[7] In PFO, other crystalline and noncrystalline phases have been identified.[8−10] Some of these phases may coexist in a solid sample, each showing specific spectral signatures.

Similar ordered states to that of PFO β-phase have been observed in other polyfluorene homopolymers,[11−13] but the stability and formation yield of such ordered domains are dependent on the length and structure of the solubilizing side groups, *n*-octyl being the most efficient one.

The origin of the mechanism leading to such high ordered states in polyfluorene homopolymers is still a matter of debate. The investigation of other systems, in particular of polyfluorene copolymers, is therefore of significant relevance.

Poly(9,9-dioctylfluorene-*alt*-bithiophene), F8T2 (Chart 1), has gained recognition as an exceptionally promising material for OFETs.[14,15] Previous studies have addressed its operational stability,[16] and protocols have been developed to produce films of highly organized character.[15,17−19] In particular, chain alignment of conjugated polymers has been shown to lead to significant increase of charge carriers' mobility.[15] The manipulation of liquid crystalline phases to achieve such high ordering in polymeric and oligomeric semiconductors has been reported.[15,20] In F8T2, macroscopic alignment after annealing in the nematic LC phase above 265 °C produces directional layers.[21] Moreover, epitaxial growth can be achieved via alignment layers.[15,22] At variance with extensive photophysical studies for a large variety of polyfluorenes, in particular PFO, a thorough examination of F8T2 photophysics is lacking.[23]

In this work we report a thermally induced conformational transition for F8T2 in solution, resembling the β-phase formation of PFO. We also report on the findings of F8T2 photophysics in the excited state and present evidence of conformational relaxation.

Experimental Section

Samples. F8T2, with $M_n = 22\,400$ and $M_w = 38\,500$ (PD = 1.7), was synthesized by a Suzuki coupling of the two comonomers. Decalin (Riedl-deHäen), methylcyclohexane (Fluka), and cyclohexane (Labscan) of spectroscopic purity grade were used without further purification. F8T2 solutions were prepared with concentrations in the 10^{-5} M range (based on monomer unit).

*Corresponding author. E-mail: macanita@ist.utl.pt.

Published on Web 12/28/2009

Chart 1

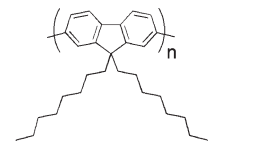

PFO
Poly(9,9-dioctylfluorene)

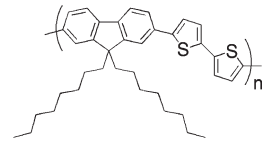

F8T2
Poly(9,9-dioctylfluorene-*alt*-bithiophene)

Methods. UV−vis absorption spectra were recorded on a Beckman DU-70 spectrophotometer. Fluorescence spectra were measured using a SPEX Fluorolog 212I spectrofluorimeter, in the S/R mode, and corrected for optics and detector wavelength dependence, except for the anisotropy measurements. For fluorescence anisotropy measurements, the excitation was vertically polarized and the emission was collected parallel $I_{\parallel}$ and perpendicular $I_{\perp}$ to the excitation (Glan-Thompson polarizers). The steady-state anisotropy $\bar{r}$ was calculated with eq 1, where G is the ratio of the instrument response to vertically and horizontally polarized light.

$$\bar{r} = \frac{I_{\parallel} - GI_{\perp}}{I_{\parallel} + 2GI_{\perp}} \quad (1)$$

The fluorescence decays were measured with the time-correlated single photon counting technique. The pumping system consists of a Millennia Xs/Tsunami lasers system from Spectra Physics, operating at 82 MHz, frequency-doubled to produce horizontally polarized pulses with 2 ps fwhm. The polarization of the excitation beam was rotated to vertical by first depolarized and then vertically polarizing (Glan-Thompson polarizer). The sample emission was collected at the magic angle (Glan-Thompson polarizer), passed through a monochromator (Jobin-Yvon H20 Vis), and detected with a microchannel plate photomultiplier (Hamamatsu R3809u-50). The R3809u-50 output pulses were used as the start pulses for a SPC acquisition module (Becker & Hickl GmbH, SPC-630). The Tsunami pulses were monitored with a fast photodiode (Becker & Hickl, GmbH) and used as the stop pulses for the SPC-630.[24] The fluorescence decays were deconvoluted from the excitation pulse using G. Striker's Sand program.[25]

Results

Absorption Spectra. At room temperature (24.6 °C, Figure 1), the absorption spectrum of F8T2 in methylcyclohexane (MCH) has a maximum at 452 nm with a characteristic shoulder at ca. 490 nm (Figure 1). The substantial red shift of the wavelength maximum with respect to those of both PFO (381 nm in MCH)[26] and dithiophene (303 nm in MCH)[27] indicates strong conjugation of the fluorene and dithiophene moieties.

Increasing the temperature up to 89 °C induces a significant blue shift of the spectrum, with loss of vibrational structure, while decreasing the temperature (−70 °C) has the opposite effect. In decalin, similar observations were made (Supporting Information).

On the other hand, the absorption spectrum of F8T2 in poor solvents (e.g., ethanol), at room temperature, resembles the low-temperature spectra in MCH. This indicates that the spectral changes observed in MCH on lowering the temperature (red shift and better vibrational resolution) are not simple temperature effects of increasing the solvent refractive index reducing inhomogeneous broadening.

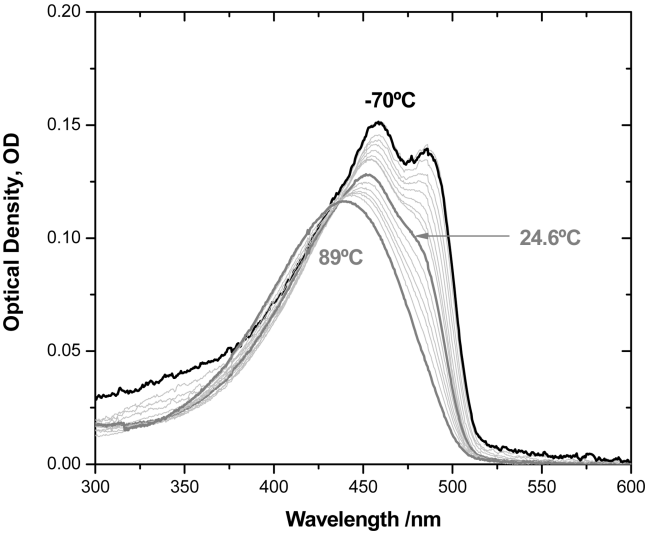

Figure 1. Absorption spectra of F8T2 in the temperature range 89 °C (gray) to −70 °C (black) with 10 °C increments in methylcyclohexane (dark gray for 24.6 °C). The spectra are corrected for the concentration change with temperature.

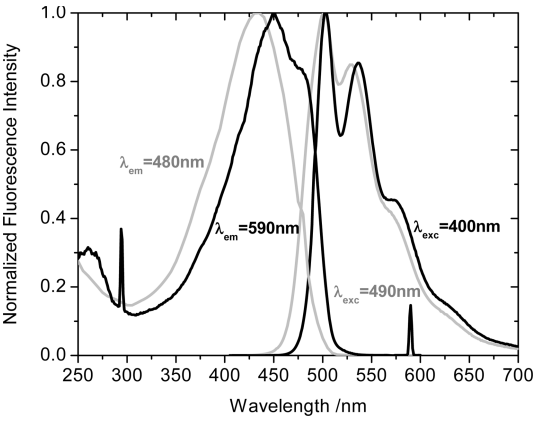

Figure 2. Fluorescence excitation (left) and emission (right) spectra of F8T2 in methylcyclohexane (MCH) at 20 °C. Excitation spectra were obtained with emission wavelengths at 480 nm (gray) and 590 nm (black), and emission spectra were obtained with excitation at 400 nm (gray) and 490 nm (black).

Fluorescence Spectra. The shape of the fluorescence spectra (emission and excitation) of F8T2 depends upon the excitation and emission wavelength, respectively (Figure 2). At 20 °C, the emission spectrum shows a slight red shift and narrowing with increasing excitation wavelength from 400 to 490 nm. The excitation spectrum is broad and unresolved when fluorescence collection is made at the onset of the emission band (480 nm). Conversely, when the fluorescence is collected at the band tail (590 nm), the spectrum shows the two first vibronic transitions that are observed in the absorption spectrum, at room temperature. The wavelength dependence of the emission and excitation spectra indicates the presence of at least two different species that absorb and emit at different wavelengths.

The shapes of the fluorescence emission and excitation spectra of F8T2 also strongly depend on temperature. Figure 3 shows the temperature effect on the emission

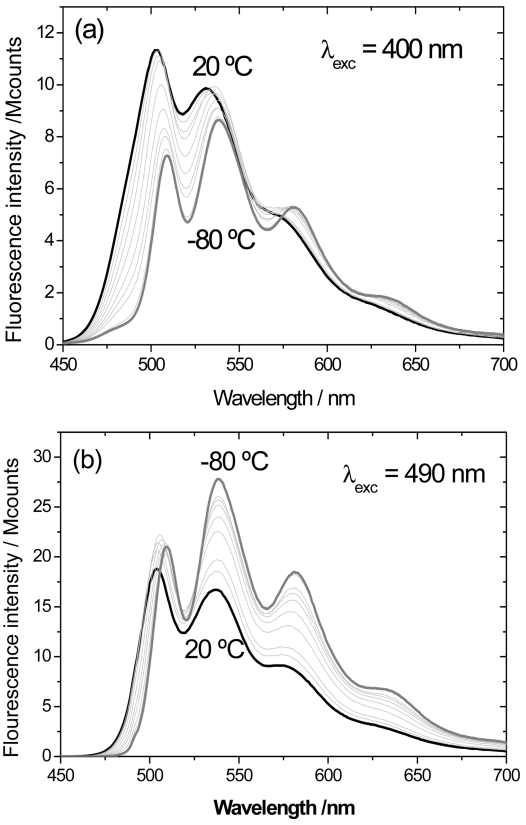

Figure 3. Emission spectra of F8T2 in MCH with (a) λ_{exc} = 400 nm and (b) λ_{exc} = 490 nm with decreasing temperature (taken at 10 °C intervals) from 20 °C (black) to −80 °C (dark gray).

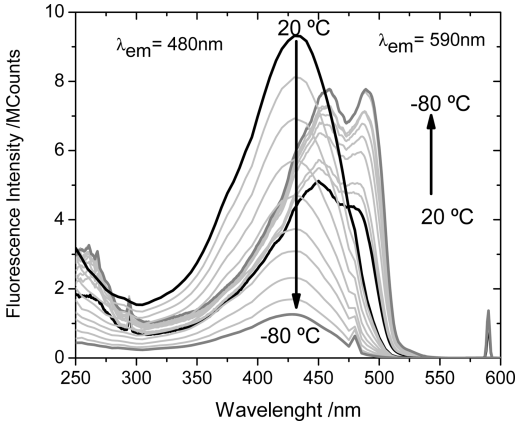

Figure 4. Excitation spectra of F8T2 in MCH with λ_{em} = 480 nm (left) and λ_{em} = 590 nm (right) with decreasing temperature at 10 °C intervals from 20 °C (black) to −80 °C (gray).

spectra obtained with the two excitation wavelengths of Figure 2: 400 nm (a) and 490 nm (b). Upon decreasing the temperature from 20 to −80 °C the spectra show a progressive decrease in intensity of the first vibronic peak and increased prominence of the second vibronic band. At −80 °C, the emission spectra obtained with excitation at 400 and 490 nm (in gray) become practically the same.

The temperature effect on the excitation spectra monitored at two different emission wavelengths at the onset (480 nm) and tail (590 nm) of the band is shown in Figure 4.

With the emission monitored at 480 nm, the excitation spectrum corresponds, at all temperatures, to the broad absorption band observed at 89 °C (Figure 1) with maximum

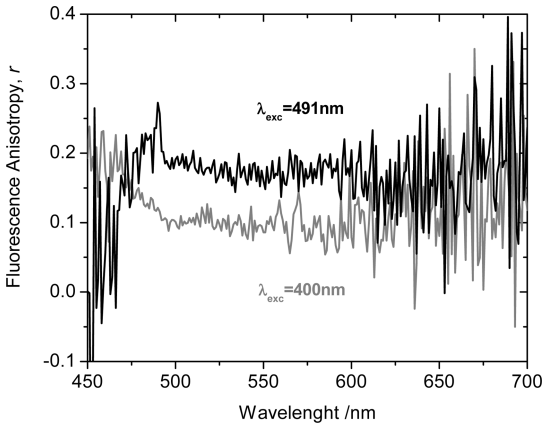

Figure 5. Steady-state fluorescence anisotropy ($\bar{r}$) traces of F8T2 in decalin, at 20 °C, measured with λ_{ex} = 400 nm (gray) and λ_{ex} = 491 nm (black).

at 440 nm and decreases in intensity on lowering the temperature. On the other hand, by monitoring the emission at 590 nm, the excitation spectrum progressively red shifts and acquires vibrational resolution upon decreasing the temperature. Identical observations were made in decalin (Supporting Information). The fact that the two excitation spectra, obtained at −80 °C with emission at 480 and 590 nm (gray spectra), are totally different from each other confirms the presence of at least two different species that absorb and emit at different wavelengths.

Summarizing the foregoing observations, (1) the absorption spectrum changes drastically with temperature (Figure 1), (2) the fluorescence spectrum depends on the excitation wavelength, shifting to the red and changing the vibrational structure at longer excitation wavelengths, (3) the excitation spectrum collected at longer emission wavelengths is vibrationally resolved and red-shifted when compared to those collected at shorter emission wavelengths, and finally (4) the temperature dependence of the fluorescence emission and absorption spectra confirms the prevalence of the structured red-shifted spectrum at low temperature and the opposite for high temperatures. Thus, we tentatively assign the high-temperature absorption and fluorescence spectra to random conformations of polymer chain segments and those same spectra observed at low temperature to more planar/ordered local conformations.[5] We will herein call these conformations the A-conformation and B-conformation, respectively.

Fluorescence Anisotropy. Fluorescence anisotropy of F8T2, in decalin at 20 °C, was measured with excitation at 400 nm (predominant absorption of the A-conformation) and at 491 nm (predominant absorption of the B-conformation). The steady-state anisotropy trace resulting from excitation at 400 nm shows a value of ca. 0.16 at the onset of the emission spectrum, which decreases to an average value around $\bar{r}$ = 0.09 at 500 nm, and thereon remains constant (gray spectrum in Figure 5). This low value indicates efficient depolarization of the fluorescence. On the other hand, the anisotropy trace obtained with excitation at 491 nm (dominant absorption of the B-conformation) shows uniformly larger values (ca. 0.18), from the emission band onset to ca. 600 nm (Figure 2).

This excitation wavelength effect on the fluorescence anisotropy resembles that observed with PFO, in which case the excitation at longer wavelengths also induced larger $\bar{r}$ values due to the presence of the β-phase.[5] In the case of PFO, it was possible to excite exclusively the β-phase and measure a steady-state anisotropy value ($\bar{r}$ = 0.35 in MCH

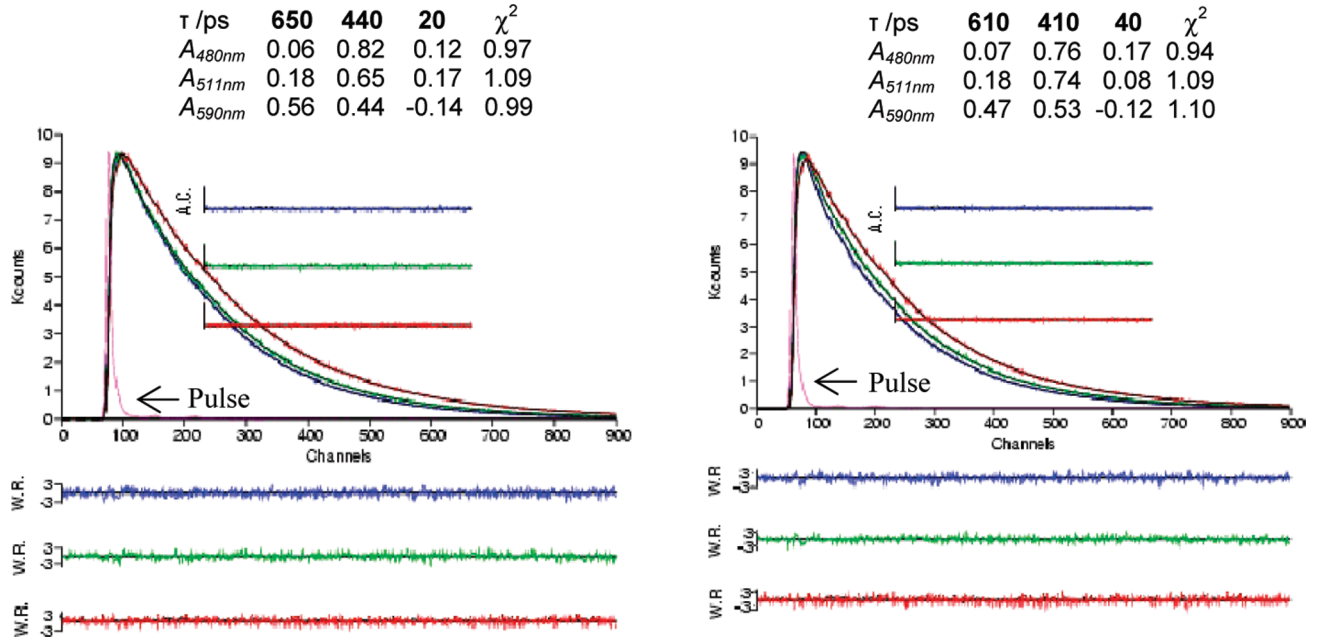

Figure 6. Global fits of the fluorescence decays of F8T2, measured at three emission wavelengths (480 nm, blue; 511 nm, green; and 590 nm, red) in MCH (left) and in decalin (right), with sums of three exponential terms. The excitation wavelength was $\lambda_{exc} = 437$ nm. The weighted residuals (W.R.), autocorrelation functions (A.C.), reduced chi-squared (χ^2) and the pre-exponential coefficients (A) are also shown.

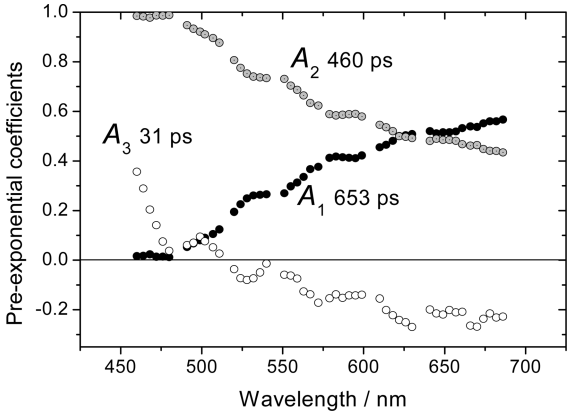

Figure 7. Pre-exponential coefficients obtained from global analysis of all the fluorescence decays of F8T2 in cyclohexane, at 20 °C, measured over the entire spectral range. The values of the pre-exponential coefficients were divided by $A_1 + A_2$.

at 20 °C) close to the anisotropy limit, consistent with the highly ordered and rigid structure[35] of the β-phase.[5] With F8T2, exclusive excitation of the B-conformation is not possible (at 20 °C), and the anisotropy change is smaller. However, it is sufficiently large to indicate a higher order of the B-conformation as compared to the A-conformation.

Time-Resolved Fluorescence. Fluorescence decays of F8T2 in MCH and decalin were measured at several emission wavelengths of the fluorescence spectrum from 460 to 686 nm. Figure 6 shows global analysis of three decays measured at representative emission wavelengths in the two solvents: the onset (480 nm), first vibronic (511 nm), and tail (590 nm) of the spectrum. The decays are triple exponentials with decay time values of 650, 440, and 20 ps in MCH, and 610, 410, and 40 ps in decalin.

Figure 7 shows the pre-exponential coefficients resulting from fitting the fluorescence decays, measured in cyclohexane (CH) at 20 °C as a function of the emission wavelength, with sums of three exponentials. The pre-exponential coefficient A_1 of the longest time ($\tau_1 = 653$ ps) is close to zero from 460 to ca. 480 nm, and increases up to 0.57 at 686 nm, while that of the middle decay time (A_2) decreases from ca. 1 to 0.43 at 686 nm. Thus, on the basis of the foregoing spectral data, we propose the assignment of the longer decay time (610 or 650 ps) to the B-conformation (absorbing and emitting at longer wavelengths) and the shorter lifetime (410 or 460 ps) to the A-conformation (absorption and emission at shorter wavelengths) for decaline and methylcyclohexane, respectively.

The shortest time ($\tau_3 = 31$ ps) is a decay time (positive pre-exponential coefficient, $A_3 > 0$) from 460 to 515 nm and a growing in ($A_3 < 0$) at longer wavelengths, meaning that part of the emission at short wavelength generates part of the emission at longer wavelengths. This behavior can a priori result from solvent/conformational relaxation[28] or intramolecular energy transfer from nonordered to ordered chain segments[29] (see Discussion).

The fluorescence decay times and pre-exponential coefficients of F8T2 in MCH were also measured at three emission wavelengths (480, 511, and 590 nm), with excitation at 434 nm, as a function of temperature (Supporting Information). Decreasing the temperature from 19 °C to −45 °C induces two relevant changes in the decays. First, the shortest decay time τ_3 increases from 21 to 46 ps, which indicates that τ_3 is associated with an activated process (Figure 8a). Second, the pre-exponential coefficient A_1 of the longest decay time (probably associated with the B-conformation) at 590 nm increases from ca. 0.5 to ca. 0.7, and A_2 decreases from 0.5 to ca. 0.3 (Figure 8b). The second observation seems to support our tentative assignment of τ_1 and τ_2 to the B- and A-conformations, respectively.

Discussion

The foregoing data indicate the presence of two conformational changes in F8T2: one occurring in the ground state as a result of temperature changes (or solvent quality) and a second one occurring in the excited state, in the picoseconds time range.

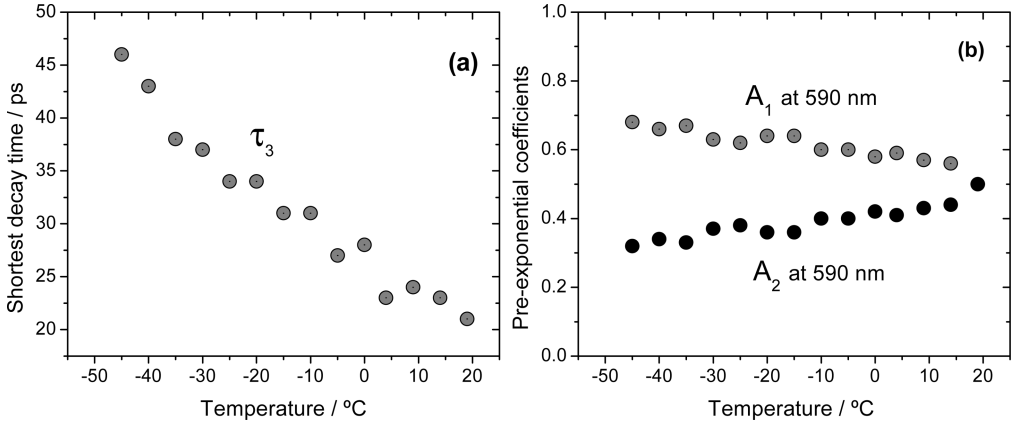

Figure 8. Data from fluorescence decays of F8T2 in MCH at several temperatures (tables in Supporting Information): (a) shortest decay time τ_3 and (b) the pre-exponential coefficients A_1 and A_2 of the two longer decay times measured at 590 nm.

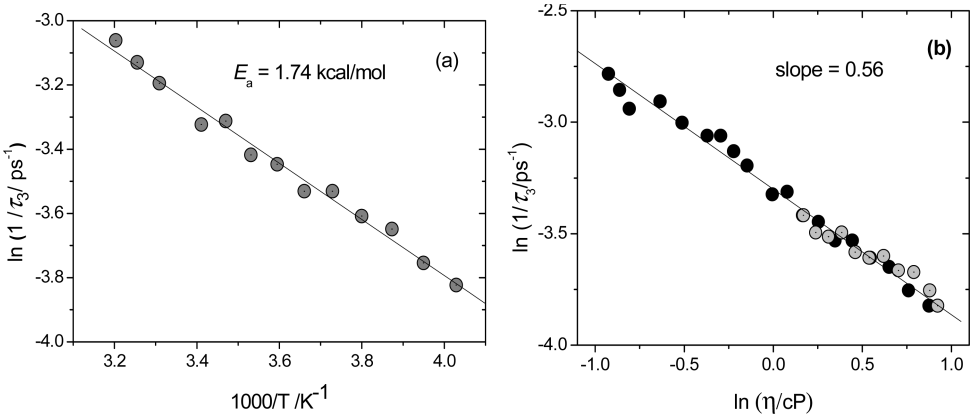

Figure 9. Arrhenius plot of (a) the reciprocal short time $1/\tau_3$ in MCH and (b) log−log plot of $1/\tau_3$ vs solvent viscosity including data at different temperatures in MCH (black) and decalin (gray). The overlap of MCH and decalin data in (b) shows that the value of τ_3 depends exclusively on viscosity independently from solvent and temperature.

Conformational Relaxation. The presence of a short fluorescence decay and growing in, appearing respectively at the onset and tail of the emission spectrum, indicates the presence of solvent and/or conformational relaxation, or intramolecular energy transfer from nonordered to ordered chain segments, or both.[28,29] The solvent viscosity and temperature effects on the short time are a signature of conformational relaxation but do not exclude energy transfer.[30] Figure 9 shows the Arrhenius plot of the reciprocal short time $1/\tau_3$ in MCH and a log−log plot of $1/\tau_3$ vs solvent viscosity including data in MCH and decalin.

From the Arrhenius plot (Figure 9a), an activation energy E_a = 1.74 kcal/mol is obtained for MCH, identical to values obtained in MCH for PFO (ca. 2 kcal/mol)[5] and for phenylenevinylene trimers (1.7 kcal/mol)[28,31] (in which energy transfer cannot occur), all having eight-carbon lateral chains (with the same van der Waals volume). Moreover, the linearity of the log−log plot shows that the relaxation rate is proportional to the reciprocal of the solvent viscosity; i.e., it is solvent viscosity controlled. The slope value is lower than unity, as previously found[32] and rationalized[33] in other systems. The two observations indicate that solvent/conformational relaxation is the principal cause for the presence of the short decay/rise times in the fluorescence decays of F8T2.

The presence of conformational relaxation in F8T2 is at first sight surprising because the bithiophene unit does not bear lateral chains, and without lateral chains the solvent friction is practically absent, leading to fast downhill relaxation. However, the "free" bithiophene motion permits coplanarization with only one of the two adjacent fluorene units, which does not suffice for extended planarization of the chain. This would always require rotations of several fluorene units.

Temperature-Induced Self-Organization. In order to characterize the ground-state conformational change of F8T2, the mole fraction of the B-conformation (x_B) was evaluated as a function of temperature, from the absorption spectra of the B-conformation, obtained from spectral decomposition of the absorption spectra shown in Figure 1. Spectral decomposition was carried out by assuming that the mole fraction of the B-conformation is equal to unity at −70 °C and equal to zero at 89 °C, i.e., $x_B(T) = \mathrm{OD}(T)/\mathrm{OD}(-70\ ^\circ\mathrm{C})$. Figure 10 shows the plot of $x_B(T)$ vs temperature. The pattern of this plot does not change when the total polymer concentration is changed (increased), ruling out significant aggregation.

Under the assumption that each conformational transition is independent from all the others we can write

$$\mathrm{A} \overset{K}{\rightleftharpoons} \mathrm{B} \qquad (2)$$

where K is the equilibrium constant of formation of the B-configuration. A similar approach has been used to analyze the formation of the PFO β-phase in the preaggregation regime.[5] The equilibrium constant, K, is then given by eq 3 and can be related to the enthalpy ΔH, entropy ΔS, and specific heat capacity ΔC_p changes, using the Gibbs−Helmholtz equation (eq 4)[34] to derive eq 5, where

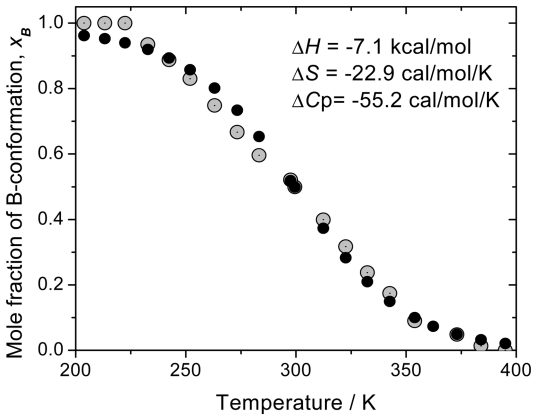

Figure 10. Mole fraction of the B-conformer x_B as a function of temperature. The gray circles represent the experimental values, and the black circles are the result of fitting the data with eq 5.

Table 1. Values of Enthalpy (ΔH^{T_m}) and Entropy (ΔS^{T_m}) at the Transition Temperature (T_m) and Specific Heat Capacity (ΔC_p) for the A- to B-Conformation Transition of F8T2 and for the α- to β-Phase Transition of PFO, Both in MCH

	ΔH^{T_m}/kcal/mol	ΔS^{T_m}/cal/(mol K)	ΔC_p/cal/(mol K)	T_m/K
F8T2	−7.06	−23.6	−55.2	299
PFO[a]	−18	−68.4		263

[a]Data from ref 5.

ΔH^{T_m} is the enthalpy change at the transition temperature T_m ($T_m = \Delta H^{T_m}/\Delta S^{T_m}$).

$$K = \frac{x_B}{1 - x_B} \tag{3}$$

$$\Delta G = \Delta H^{T_m}\left(1 - \frac{T}{T_m}\right) + \Delta C_p\left[(T - T_m) - T \ln \frac{T}{T_m}\right] \tag{4}$$

$$R \ln K = \left(\frac{\Delta H^{T_m}}{T_m} - \Delta C_p(1 + \ln T_m)\right) + (\Delta C_p T_m - \Delta H^{T_m})\frac{1}{T} + \Delta C_p \ln T \tag{5}$$

The minimization of the weighted deviations of the experimental and calculated values of x_B [$wd = (x_B^{exp} - x_B^{cal})^2/x_B^{exp}$)] was achieved by the iteration of the enthalpy (ΔH^{T_m}), specific heat capacity (ΔC_p), and transition temperature (T_m) values. The results are compared to those obtained for PFO β-phase formation in Table 1.

The negative values of both ΔH^{T_m} and ΔS^{T_m} indicate that the A- to B-conformation transition is exothermic with substantial entropy loss, as expected for a transition from a less ordered to more ordered conformation. The less pronounced enthalpy and entropy changes of F8T2 as compared to those observed with PFO indicate that the B-conformation is less ordered than the PFO β-phase, as the milder spectral changes observed with F8T2 suggest. In the case of polyalkylfluorenes, it was shown that the β-phase is a quasi-planar conformation of the polymer resulting from the alignment of the lateral chains with the backbone.[31,10] The necessary matching of chain length and available space in the backbone is optimal for alkyl = *n*-octyl, i.e., for PFO. The milder transition observed with F8T2 is thus attributed to the presence of the bithiophene units that, although having approximately the same size as the fluorene unit, do not bear the octyl side chains.

The isotropic domain of F8T2 is currently used, through annealing, in the production of aligned layers for electronic devices.[14,15] However, the current understanding of the dynamics of F8T2 in solution suggests a possible transfer of a preferential B-conformation onto films. Therefore, some parallelism between the reported liquid crystalline phases of F8T2 in the solid state[18] and the A- and B-conformations in solution may exist.

Conclusions

F8T2 shows conformational relaxation (ca. 27 ps in CH at 20 °C) in the excited state, joining the growing number of polymers and oligomers bearing side chains that show this kind of process. In the ground state, F8T2 undergoes a temperature-induced transition between differently ordered conformations, the more ordered conformation resembling the β-phase conformation of PFO.

Acknowledgment. Fundação para a Ciência e Tecnologia (FCT) is acknowledged for project funding (POCI/CFM/58767/2004) and also for the doctoral grant of R.F.R. (SFRH/BD/27908/2006).

Supporting Information Available: Fluorescence emission and excitation spectra of F8T2 in decalin and time-resolved fluorescence data in methylcyclohexane. This material is available free of charge via the Internet at http://pubs.acs.org.

References and Notes

(1) Forrest, S. R. *Nature* **2004**, *428*, 911–918.
(2) Chua, L. L.; Zaumseil, J.; Chang, J. F.; Ou, E. C. W.; Ho, P. K. H.; Sirringhaus, H.; Friend, R. H. *Nature* **2005**, *434*, 194–199.
(3) Bradley, D. D. C.; Grell, M.; Long, X.; Mellor, H.; Grice, A.; Inbasekaran, M.; Woo, E. P. *Proc. SPIE* **1997**, *3145*, 254–259.
(4) Grell, M.; Bradley, D. D. C.; Long, X.; Chamberlain, T.; Inbasekaran, M.; Woo, E. P.; Soliman, M. *Acta Polym.* **1998**, *49*, 439–444.
(5) Dias, F. B.; Morgado, J.; Maçanita, A. L.; Costa, F. P.; Burrows, H. D.; Monkman, A. P. *Macromolecules* **2006**, *39*, 5854–5864.
(6) Da Como, E.; Becker, K.; Feldmann, J.; Lupton, J. M. *Nano Lett.* **2007**, *7*, 2993–2998.
(7) Changfeng, W.; McNeill, J. *Langmuir* **2008**, *24*, 5855–5861.
(8) Chen, S. H.; Su, A. C.; Chen, S. A. *J. Phys. Chem. B* **2005**, *109*, 10067–10072.
(9) Chen, S. H.; Su, A. C.; Su, C. H.; Chen, S. A. *Macromolecules* **2005**, *38*, 379–385.
(10) Chunwaschirasiri, W.; Tanto, B.; Huber, D. L.; Winokur, M. J. *Phys. Rev. Lett.* **2005**, *94*, 107402.
(11) Teetsov, J.; Bout, D. A. V. *Langmuir* **2002**, *18*, 897–903.
(12) Knaapila, M.; Dias, F. B.; Garamus, V. M.; Almasy, L.; Torkkeli, M.; Leppanen, K.; Galbrecht, F.; Preis, E.; Burrows, H. D.; Scherf, U.; A. P.; Monkman, A. P. *Macromolecules* **2007**, *40*, 9398–9405.
(13) Bright, D. W.; Dias, F. B.; Galbrecht, F.; Scherf, U.; Monkman, A. P. *Adv. Funct. Mater.* **2009**, *19*, 67–73.
(14) Salleo, A.; Street, R. A. *Appl. Phys. Lett.* **2002**, *81*, 2887–2889.
(15) Sirringhaus, H.; Wilson, R. J.; Friend, R. H.; Inbasekaren, M.; Wu, W.; Woo, E. P.; Grell, M.; Bradley, D. D. C. *Appl. Phys. Lett.* **2000**, *77*, 406–408.
(16) Jo, J.; Vak, D.; Noh, Y. Y.; Kim, S. S.; Lim, B.; Kim, D. Y. *J. Mater. Chem.* **2008**, *18*, 654–659.
(17) Gather, M. C.; Bradley, D. D. C. *Adv. Funct. Mater.* **2007**, *17*, 479–485.
(18) Pattison, L. R.; Hexemer, A.; Kramer, E. J.; Krishnan, S.; Petroff, P. M.; Fischer, D. A. *Macromolecules* **2006**, *39*, 2225–2231.
(19) Surin, M.; Sonar, P.; Grimsdale, A. C.; Müllen, K.; Lazzaroni, R.; Leclère, P. *Adv. Funct. Mater.* **2005**, *15*, 1426–1434.
(20) Shimizu, Y.; Oikawa, K.; Nakayama, K.; Guillon, D. *J. Mater. Chem.* **2007**, *17*, 4223–4229.

(21) Grell, M.; Redecker, M.; Whitehead, K. S.; Bradley, D. D. C.; Inbasekaren, M.; Woo, E. P.; Wu, W. *Liq. Cryst.* **1999**, *26*, 1403–1407.
(22) Banach, M. J.; Friend, R. H.; Sirringhaus, H. *Macromolecules* **2003**, *36*, 2838–2844.
(23) Lin, H. C.; Sung, H. H.; Tsai, C. M.; Li, K. C. *Polymer* **2005**, *46*, 9810–9820.
(24) Rodrigues, R. F.; Silva, P. F.; Shimizu, K.; Freitas, A. A.; Kovalenko, S. A.; Ernsting, N. P.; Quina, F. H.; Maçanita, A. *Chem.—Eur. J.* **2009**, *15*, 1397–1402.
(25) Striker, G.; Subramanian, V.; Seidel, C. A. M.; Volkmer, A. *J. Phys. Chem. B* **1999**, *103*, 8612–8617.
(26) Dias, F. B.; Maçanita, A. L.; Melo, J. S.; Burrows, H. D.; Guntner, R.; Scherf, U.; Monkman, A. P. *J. Chem. Phys.* **2003**, *118*, 7119–7126.
(27) Becker, R. S.; Melo, J. S.; Maçanita, A. L.; Elisei, F. *Pure Appl. Chem.* **1995**, *67*, 9–16.
(28) Di Paolo, R. E.; Melo, J. S.; Pina, J.; Burrows, H. D.; Morgado, J.; Maçanita, A. L. *ChemPhysChem* **2007**, *8*, 2657–2664.
(29) Bredas, J. L.; Beljonne, D.; Coropceanu, V.; Cornil, J. *Chem. Rev.* **2004**, *104*, 4971–5003.
(30) Vaughan, H. L.; Dias, F. M. B.; Monkman, A. P. *J. Chem. Phys.* **2005**, *122*, 014902.
(31) Di Paolo, R. E.; Gigante, B.; Esteves, M. A.; Pires, N.; Santos, C.; Lameiro, M. H.; Melo, J. S.; Burrows, H. D.; Maçanita, A. L. *ChemPhysChem* **2008**, *9*, 2214–2220.
(32) Velsko, S. P.; Fleming, G. R. *J. Chem. Phys.* **1982**, *76*, 3553–3562.
(33) Grote, R. F.; Hynes, J. T. *J. Chem. Phys.* **1981**, *74*, 4465–4475.
(34) Levine, I. N. *Physical Chemistry*, 5th ed.; McGraw-Hill: New York, 2003.
(35) A value of $\bar{r}$ close to the limit r_0 (fundamental anisotropy 0.4) implies that all the decay times of the anisotropy decay, τ_i, are much longer than the chromophore lifetime τ_0 and, thus, indicate substantial rigidity for the B-conformation.